

# Investigation of Bluff Body Size Effects on Piezoelectric Performance Using Flow-Induced Vibration <sup>†</sup>

Muhammad Mahad Shah <sup>1,2,\*</sup>, Moeen Mahboob <sup>2</sup>, Usman Latif <sup>1</sup>, Emad Uddin <sup>1</sup>, Muhammad Rizwan Siddiqui <sup>1,3</sup> and Muhammad Zulfiqar <sup>1,3</sup>

<sup>1</sup> Department of Mechanical Engineering, School of Mechanical and Manufacturing Engineering, National University of Sciences and Technology, Islamabad 44000, Pakistan; emaduddin@smme.nust.edu.pk (E.U.); rizwan.siddiqui@cust.edu.pk (M.R.S.); muhammad.zulfiqar@cust.edu.pk (M.Z.)

<sup>2</sup> Department of Mechanical Engineering, HITEC University, Taxila 47080, Pakistan; moeen.mahboob@hitecuni.edu.pk

<sup>3</sup> Department of Mechanical Engineering, Capital University of Science and Technology, Islamabad 45750, Pakistan

\* Correspondence: mahad.phd19smme@student.nust.edu.pk

<sup>†</sup> Presented at the 4th International Conference on Advances in Mechanical Engineering (ICAME-24), Islamabad, Pakistan, 8 August 2024.

**Abstract:** An experimental analysis of the effect of size variation for a cylindrical-shaped bluff body in flow-induced vibration (FIV) for the purposes of harvesting ambient energy is explored in this study. The research was conducted at a very low Reynold's number in a closed-loop tunnel operating at a very low speed. An investigation of the power generation potential achieved by varying the size of the bluff body was conducted. A comparative study is also presented for varying the diameter configuration against the distance of the energy-harvesting piezoelectric flag from the cylindrical bluff body. At distances other than the optimal distance of the piezoelectric harvester from the bluff body, reduced efficacy of the power generation is observed. The results show a 17% increase in power with the use of 2x the size of the reference bluff body.

**Keywords:** renewable energy; vortex-induced vibrations; energy harvesting; blockage ratio



**Citation:** Shah, M.M.; Mahboob, M.; Latif, U.; Uddin, E.; Siddiqui, M.R.; Zulfiqar, M. Investigation of Bluff Body Size Effects on Piezoelectric Performance Using Flow-Induced Vibration. *Eng. Proc.* **2024**, *75*, 21. <https://doi.org/10.3390/engproc2024075021>

Academic Editors: Muhammad Mahabat Khan, Muhammad Irfan, Mohammad Javed Hyder and Manzar Masud

Published: 24 September 2024



**Copyright:** © 2024 by the authors. Licensee MDPI, Basel, Switzerland. This article is an open access article distributed under the terms and conditions of the Creative Commons Attribution (CC BY) license (<https://creativecommons.org/licenses/by/4.0/>).

## 1. Introduction

As the depletion of natural resources becomes more evident, research is now moving towards alternative power sources. Limited life span, power efficacy, and energy capacity are some of the challenges we face today [1,2]. Significant effort has been dedicated to research into collecting energy from ambient sources to either do away with the need for batteries altogether or significantly increase their lifespan. Applications include, but are not limited to, biomedical sensors, health implants, and remote as well as large sensor networks [3–7]. There are a variety of energy harvesting materials available, each with its own distinct process of energy conversion. Power ranging from microwatts to milliwatts is sufficient and is the typical focus of piezoelectric energy harvesting. In certain conditions, due to the wavy/vibrational nature of the power source, piezoelectric harvesting is considered more viable than thermal and solar harvesting. These natural vibrations include civil structures, underwater areas, mammals, and moving apparatus. In general, vibrations can be effectively converted into usable energy through various methods.

Among piezoelectric harvesting techniques, extensive research is available on the active flapping of piezoelectric flags by flow-induced vibrations, especially with the design context of the FIV producing bluff body being directly attached to the energy harvesting flag [6], as depicted in Figure 1a. The bluff body in question here has varying geometries, ranging from standard geometrical shapes to NACA aerofoil [8]. For FIV energy harvesting

from a piezoelectric flag where the bluff body is detached and acts as a vortex producer, experimental research by U. Latif et al. devised an extensive experimental setup to investigate the effect of the VIV on the piezoelectric flag [9], as demonstrated in Figure 1b.

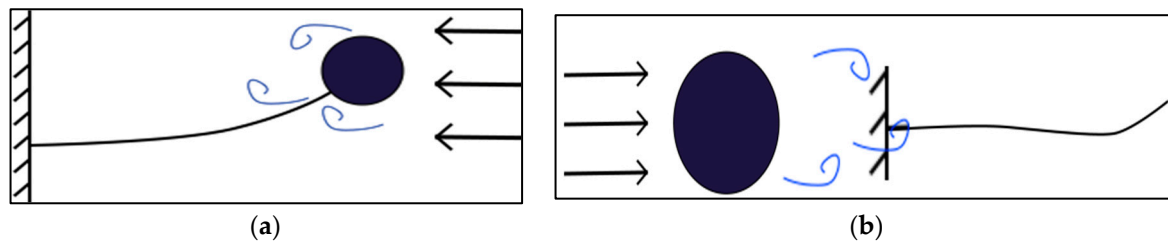


**Figure 1.** (a) Left: Attached bluff body with piezoelectric flag under flow-induced vibrations, (b) Right: Flag under VIV from the flow over the detached bluff body.

Such a dissociated cantilever mechanism for harvesting energy from a piezoelectric flag was employed to experimentally investigate the energy yield with respect to the flapping amplitude and frequency, while the bluff body in this study was an aluminum cylinder with a diameter of 25 mm [8].

It is pertinent to mention that all of the previous studies been focused on achieving the flutter at a low speed for energy harvesting systems. In these studies, the setups designed to capture this energy are an important part of the study, hence with an experimental aim of finding an energy harvesting mechanism that can operate effectively across a wide range of high wind speeds [10,11]. Galloping is a type of self-limiting and self-excited cycle system that has the ability to stimulate a mechanical energy harvester through increased oscillation amplitude at a low frequency of vortex shedding or low wind speed [12]. Galloping is also believed to be suitable for MEMS harvesters [13] that possess high stiffness to withstand the weight of the bluff body and can effectively withstand significant deflection of the harvester. The upgraded iteration of the galloping mechanism is referred to as the wake galloping configuration. Another study published a configuration in which two bluff bodies were used to harvest energy. One bluff body was fixed at the head of the flag and the other bluff body was moved downstream at different distances from the flag to investigate their effect on harvested energy [14]. Another recent publication explored the energy harvesting potential of a pivoted cantilever mechanism for a piezoelectric flag in a velocity range of 0.1–0.3 m/s, while also investigating the tandem arrangement of bluff bodies of the same size [15].

Considering a piezoelectric flag placed under such an arrangement for the sole purpose of energy harvesting, parameters such as the geometrical shape of the blunt body, the type of FIV, and the distance of the flag from the blunt body are of the utmost importance for forming a meaningful correlation with the optimal energy output [16]. Among these parameters, the dependency of the power generated upon the size of the bluff body, while keeping all the other parameters constant, is an area that still needs to be explored.

In this study, a comprehensive experimental investigation has been conducted on the effect of the size of the bluff body. To fully understand this effect, the energy harvesting potential of the same bluff body of two different sizes has been explored in this study. Our setup of interest is a piezoelectric flag mounted behind a circular bluff body where it flutters under FIV in the wake of the flow. In our experimental investigation setup, two cylinders of the same material and the same geometry were used in independent experiments where the size of one cylinder is twice that of the other. The energy harvesting potential is expected to illustrate the effect of an increment in the size of the cylinder used as the bluff body in a streamline flow with a very low Reynold's number.

## 2. Experimental Setup

This study was conducted at a very low Reynold's number in a closed-loop tunnel operating at a very low speed. In Figure 2, the experimental setup is depicted schematically.

The low-velocity water tunnel has a velocity range of 0–0.5 m/s and a test section measuring 2.0 m in length, 0.4 m in width, and 0.4 m in height. The water flow equipment was driven by a centrifugal pump, and its RPM was regulated by a variable frequency drive ranging from 1 to 50 Hz, allowing the water velocity to be varied between 0 and 0.5 m/s. To make the flow uniform, a honeycomb structure with a hexagon opening made of aluminum with the dimensions 1.83 m × 0.5 m × 0.0254 m (L × W × H) was employed in the flow loop before the test section. The turbulence intensity measured was less than 1%. This manifestation of flow quality was encouraging and will thus provide us with better accuracy for experimentation.

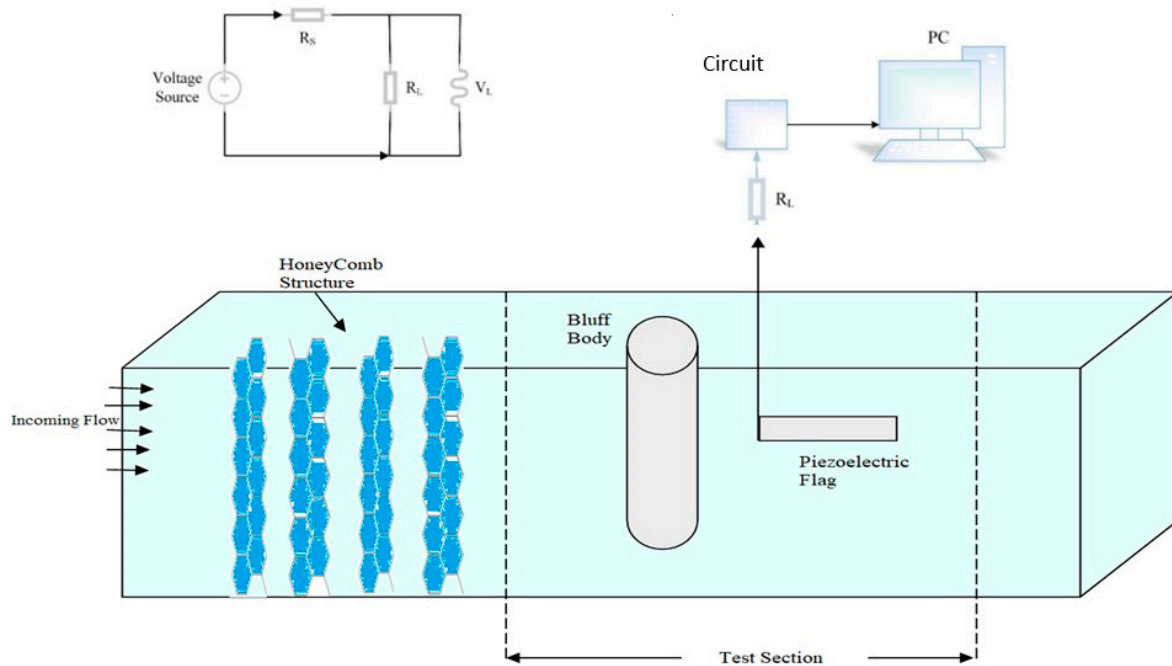


**Figure 2.** Schematic of the experimental setup.

For the observations, the Particle Image Velocimetry (PIV) tool was used to measure the free-stream velocity of the fluid, and a high-speed camera was used to record the flag's movement. Proper lighting conditions were ensured to improve the recording's visual appeal for the frame grabber. The voltage created from the piezoelectric flag was recorded by utilizing a NI-DAQ 6009USB card (National Instruments, Austin, TX, USA). MATLAB 2024 software was used to further process the recorded videos, to extract the flag's flapping envelope, and to calculate the amplitude and frequency of the vibrations.

In this investigation, the experiments were conducted on 14 different cases while all the previously mentioned characteristics and parameters remained the same with the exception of the bluff bodies. The details of the bluff bodies, with the arrangement and parameters, are showed in Table 1. Our bluff body had a hollow cylindrical arrangement made up of a circular aluminum rod, because of having a good surface finish, less roughness, and excellent machinability quality. Figures 3 and 4 show that the bluff body was fixed in the test section with the help of an adjustable traverse mechanism, and a piezo flag was placed behind the bluff body.

A sophisticated traverse mechanism was used for accurately varying the distance of the piezoelectric flag from the bluff for different  $X/D$  (ratio of the distance of the flag from the bluff body to the diameter of the bluff body) positions. The fluctuation of the flag was recorded by a camera at 50 fps from the bottom of the tunnel, as shown in Figure 3.

**Table 1.** Proposed energy harvesting parameters.

| Parameter                               | Configuration Measurement |
|---|---------------------------|
| Cylinder (bluff body)                   | 12.5 mm and 25 mm Dia     |
| Blockage ratio for 25 mm Cyl.           | 6.25%                     |
| Blockage ratio for 12.5 mm Cyl.         | 3.125%                    |
| Elastic modulus (GPa)                   | 1.38                      |
| Poisson’s ratio                         | 0.46                      |
| Density, (kg/m <sup>3</sup> )           | 1.75 × 10 <sup>3</sup>    |
| Active length of piezoelectric flag (L) | 62 mm                     |
| Width of piezoelectric flag (W)         | 12 mm                     |
| Thickness of piezoelectric flag (t)     | 52 μm                     |
| Impedance of piezoelectric flag (Z)     | 1 MΩ                      |
| Output Voltage                          | 10 mV–100 V               |
| Fluid                                   | Water                     |
| Fluid Velocity                          | 0.26 m/s                  |
| Reynold’s Number (Re)                   | 3145                      |
| Fluid density                           | 998 kg/m <sup>3</sup>     |

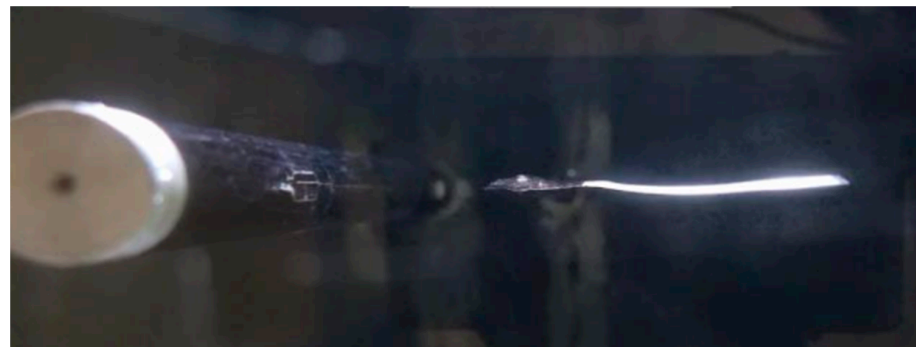


**Figure 3.** Oscillating flag behind the 25-mm diameter circular cylinder.

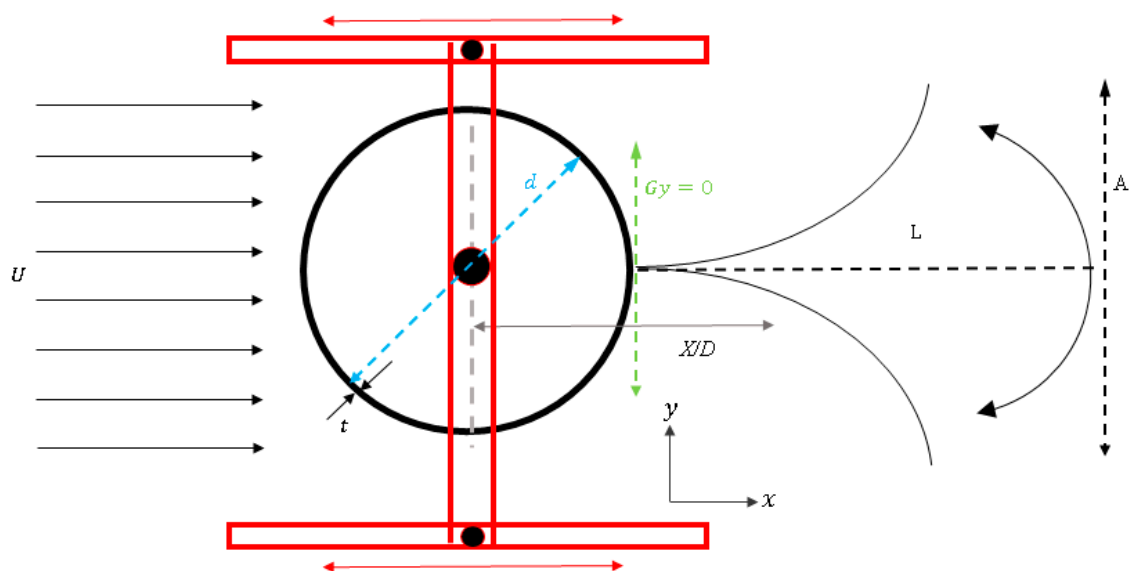


**Figure 4.** Schematic diagram of experimental cases.

### 3. Results and Discussion

The primary focus of the investigation was the flapping behavior and the parameters of amplitude (A/L) and frequency (F) as these parameters are the factors that have an impact on voltage generation and power. The formula

$$P_{out} = \frac{V_{rms}^2}{R_L} \tag{1}$$

where  $V_{rms}$  is the root mean square voltage and  $R_L$  is the load resistance, used to calculate the power output ( $P_{out}$ ). We aimed to comprehend the energy harvesting capabilities of the piezoelectric flag under low or constant flow conditions by examining these parameters for the various bluff body arrangements while maintaining a constant flow rate and cross-wise distance.

#### 3.1. Single Cylinder of 12.5 mm

By keeping the cross-wise distance constant ( $G_y = 0$ ) and the flow rate constant ( $U = 0.26$  m/s), the power responses of this case were investigated by placing the piezoelectric flag behind a single cylinder with a diameter of 12.5 mm by a stream-wise range for  $X/D = 2.0 - 5.0$ . Figure 5 shows the power response on each point. The maximum power output was achieved when the piezoelectric flag was placed at a stream-wise  $X/D = 3.0$ . The flapping response and amplitude of the case single cylinder 12.5 mm at  $X/D = 3.0$  can be seen in Figure 6. We observed that by increasing the stream-wise distance, more power is generated until the mid-point, then a sudden drop in power begins and then rises again; this is because we observed the vortex at the mid-point to be more than the vortex at the start and end of the  $X/D$  range.

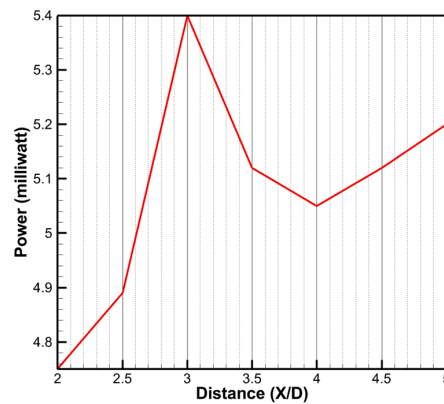


Figure 5. Power output of flag for 12.5-mm cylinder at  $U = 0.26$  m/s.

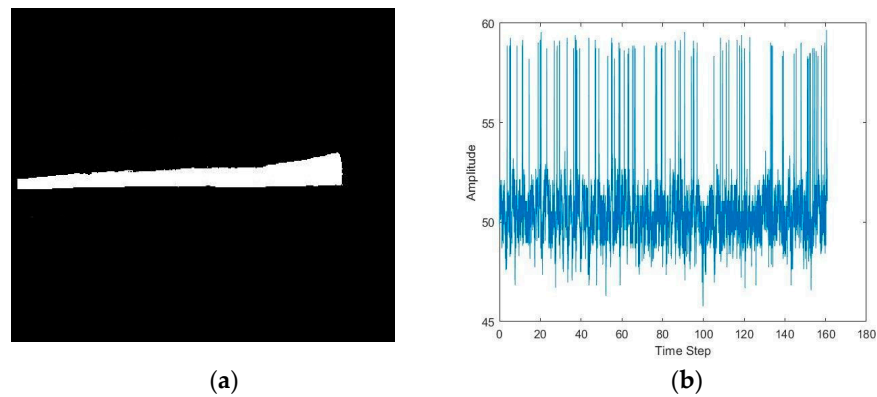


Figure 6. (a) Flapping response (b) Amplitude variation with amplitude “A” represented for  $U = 0.26$  m/s.

### 3.2. Single Cylinder of 25 mm

By keeping the cross-wise distance constant  $G_y = 0$  and the flow-rate constant  $U = 0.26$  m/s, the power responses of this case were investigated by placing the piezoelectric flag behind a single cylinder with a diameter of 12.5 mm and by varying the stream-wise distances  $X/D = 2.0 - 5.0$ . Figure 7 shows the power response on each point. The maximum power output was achieved when the piezoelectric flag was placed at a stream-wise distance  $X/D = 3.0$ . The flapping response and amplitude for the case of the single cylinder with a diameter of 25 mm at  $X/D = 3.0$  can be seen in Figure 7. The power response thus observed signifies that the vortex significance in the mid-point is more than at the ends of the  $X/D$  range.

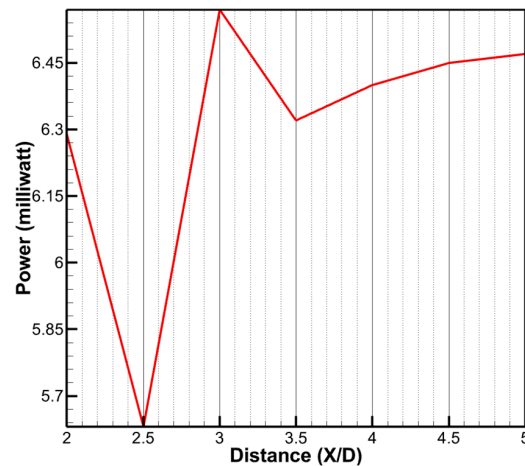


Figure 7. The power responses of 25-mm cylinder at  $U = 0.26$  m/s.

## 4. Comparison of Results

From the various cases performed, it was observed that the maximum power varies depending on the cylinder configuration and diameter. The 25-mm diameter single cylinder produced more power than the 12.5-mm diameter single cylinder and the maximum power was harvested at the  $X/D = 3$  while the power at other distances was noticed to be less in both cases.

While directly observing and comparing the flapping response profiles between the bluff bodies of diameters 12.5 mm and 25 mm, we can see that a greater amplitude of flapping response was obtained when experimenting with the latter bluff body. Moreover, the amplitude of the piezoelectric flag with a bluff body of diameter 25 mm is about 30% higher than that of the 12.5-mm bluff body, as is evident from the amplitude–time graphs represented in Figures 6b and 8b, respectively.

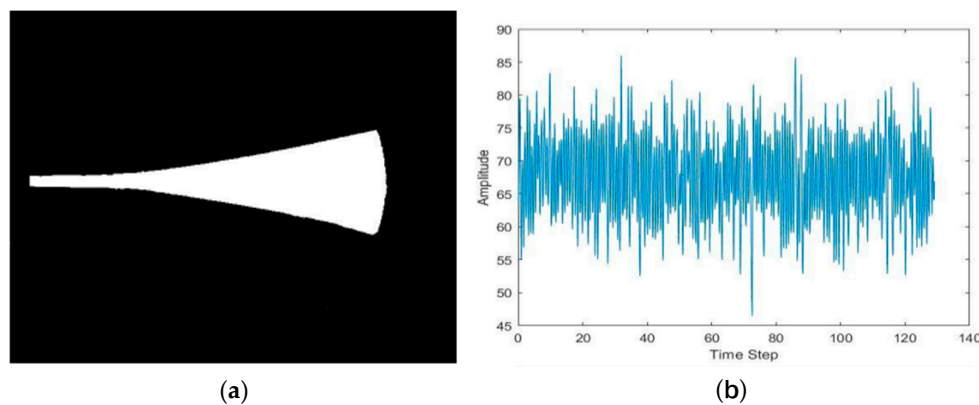
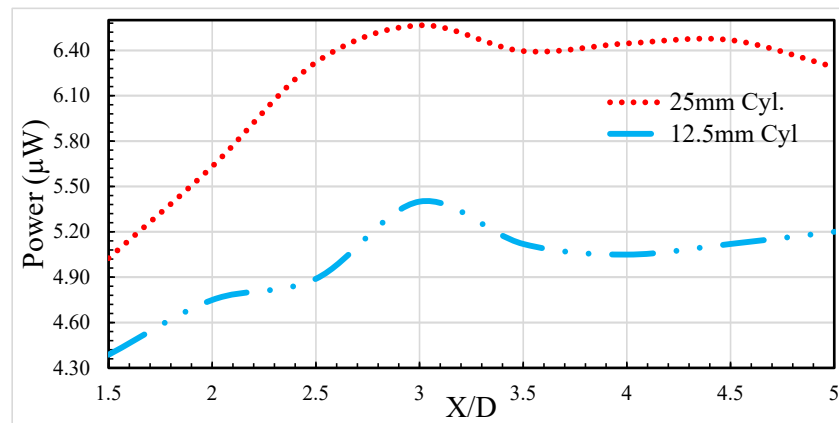


Figure 8. (a) Flapping response (b) Amplitude variation with amplitude “A” at  $X/D = 3$  &  $U = 0.26$  m/s.

The best case for a single-cylinder setup was when the piezoelectric flag was placed at a distance of  $X/D = 3.0$  from the 25-mm cylinder. This configuration maximizes the power output. Figure 9 shows the power response at each point, signifying that  $X/D = 3.0$  produced the maximum power. This configuration efficiently collected energy from the liquid flow, resulting in considerably more power generation.



**Figure 9.** Power response of both cylinders.

The worst case for a single-cylinder arrangement was observed when the upstream clearance ( $X/D$ ) deviated from the optimum value of 3.0. These results show that more power was generated as the distance downstream from the center increased, up to the optimum point, beyond which the power suddenly dropped. This suggests that if the upstream distance is too far from the optimum, the output will drop. More vortices were observed along the center of the cylinder assembly, resulting in a less favorable environment for power generation. Therefore, values of  $X/D$  outside the range of 2.0 to 5.0 can lead to suboptimal power generation and reduced efficiency.

The specific current interval to achieve maximum power varies from case to case, emphasizing the importance of optimization for different cylinder configurations. In summary, power and flow characteristics are affected by cylinder diameter, layout, and flow spacing. These insights are useful in designing and optimizing piezoelectric energy harvesting systems with different cylinder configurations.

## 5. Conclusions

In this experimental study, the dependency of the power generation of a piezoelectric flag upon FIV caused by a bluff body of varying geometrical sizes as well as the distance of the flag from the bluff body was investigated by performing a limited set of experiments. Two distinct bluff bodies of the same geometry but of different diametric sizes were used in the experiment and the observations show promising results for energy harvesting with respect to the varying distance between the flag and bluff body as well as geometric size parameters.

The findings provided by this study shed light on the complicated link that exists in piezoelectric energy harvesting devices between the power output and the flow parameters. The comparative analysis of two bluff bodies led to the conclusion that the increase in energy harvested from the use of a bluff body of 25 mm diameter is 17% more than that of one of 12.5 mm diameter, which is a remarkable increase when keeping all the other parameters the same. The information derived from this study is crucial for the process of designing and optimizing systems of this kind for a wide variety of cylinder designs, which will, ultimately, contribute to the development of sustainable energy solutions. In the future, research in this field may further investigate the connection between fluid flow dynamics and cylinder shapes in order to uncover an even higher potential for piezoelectric energy harvesting devices.

**Author Contributions:** Conceptualization, M.M.S. and E.U.; methodology, M.M.S., M.M. and U.L.; software, M.R.S.; validation, M.M.S., E.U., M.Z. and U.L.; formal analysis, M.M.S. and M.M.; investigation, M.M.S.; resources, M.M.S. and E.U.; data curation, M.M.S., M.M. and M.Z. writing—original draft preparation, M.M.S. and M.M.; writing—review and editing, M.M.S., M.M. and U.L.; visualization, E.U.; supervision, E.U.; project administration, E.U.; funding acquisition, E.U. All authors have read and agreed to the published version of the manuscript.

**Funding:** This research received no external funding.

**Institutional Review Board Statement:** Not applicable.

**Informed Consent Statement:** Not applicable.

**Data Availability Statement:** The raw data supporting the conclusions of this article will be made available by the authors upon request.

**Acknowledgments:** We extend our heartfelt gratitude to our colleagues, fellow researchers, and research scholars at the School of Mechanical and Manufacturing Engineering, NUST, for their invaluable insights and expertise, which made this work possible. Their dedication and support have been instrumental in advancing our research. Moreover, we would like to pay our thanks to NUST H12, Islamabad for allowing us to perform our experiments in the flow visualization lab of SMME.

**Conflicts of Interest:** The authors declare no conflicts of interest.

## References

1. Lu, M.; Fu, G.; Osman, N.B.; Konbr, U. Green energy harvesting strategies on edge-based urban computing in sustainable internet of things. *Sustain. Cities Soc.* **2021**, *75*, 103349. [[CrossRef](#)]
2. Song, G.J.; Cho, J.Y.; Kim, K.B.; Ahn, J.H.; Song, Y.; Hwang, W.; Hong, S.D.; Sung, T.H. Development of a pavement block piezoelectric energy harvester for self-powered walkway applications. *Appl. Energy* **2019**, *256*, 113916. [[CrossRef](#)]
3. Dunmon, J.A.; Stanton, S.C.; Mann, B.P.; Dowell, E.H. Power extraction from aeroelastic limit cycle oscillations. *J. Fluids Struct.* **2011**, *27*, 1182–1198. [[CrossRef](#)]
4. Huang, H.; Wei, H.; Lu, X.Y. Coupling performance of tandem flexible inverted flags in a uniform flow. *J. Fluid Mech.* **2018**, *837*, 461–476. [[CrossRef](#)]
5. Mutsuda, H.; Tanaka, Y.; Patel, R.; Doi, Y. Harvesting flow-induced vibration using a highly flexible piezoelectric energy device. *Appl. Ocean Res.* **2017**, *68*, 39–52. [[CrossRef](#)]
6. Sun, W.; Wang, Y.; Liu, Y.; Su, B.; Guo, T.; Cheng, G.; Zhang, Z.; Ding, J.; Seok, J. Navigating the future of flow-induced vibration-based piezoelectric energy harvesting. *Renew. Sustain. Energy Rev.* **2024**, *201*, 114624. [[CrossRef](#)]
7. Tairab, A.M.; Wang, H.; Hao, D.; Azam, A.; Ahmed, A.; Zhang, Z. A hybrid multimodal energy harvester for self-powered wireless sensors in the railway. *Energy Sustain. Dev.* **2022**, *68*, 150–169. [[CrossRef](#)]
8. Liu, J.; Zuo, H.; Xia, W.; Luo, Y.; Yao, D.; Chen, Y.; Wang, K.; Li, Q. Wind energy harvesting using piezoelectric macro fiber composites based on flutter mode. *Microelectron. Eng.* **2020**, *231*, 111333. [[CrossRef](#)]
9. Mujtaba, A.; Latif, U.; Uddin, E.; Younis, M.Y.; Sajid, M.; Ali, Z.; Abdelkefi, A. Hydrodynamic energy harvesting analysis of two piezoelectric tandem flags under influence of upstream body's wakes. *Appl. Energy* **2021**, *282*, 116173. [[CrossRef](#)]
10. Latif, U.; Dowell, E.H.; Uddin, E.; Yamin Younis, M. Parametric aerodynamic and aeroelastic study of a deformable flag-based energy harvester for powering low energy devices. *Energy Convers. Manag.* **2023**, *280*, 116846. [[CrossRef](#)]
11. Yu, Y.; Liu, Y. Flapping dynamics of a piezoelectric membrane behind a circular cylinder. *J. Fluids Struct.* **2015**, *55*, 347–363. [[CrossRef](#)]
12. Wang, J.; Geng, L.; Ding, L.; Zhu, H.; Yurchenko, D. The state-of-the-art review on energy harvesting from flow-induced vibrations. *Appl. Energy* **2020**, *267*, 114902. [[CrossRef](#)]
13. Priya, S.; Song, H.C.; Zhou, Y.; Varghese, R.; Chopra, A.; Kim, S.G.; Kanno, I.; Wu, L.; Ha, D.S.; Ryu, J.; et al. A Review on Piezoelectric Energy Harvesting: Materials, Methods, and Circuits. *Energy Harvest. Syst.* **2019**, *4*, 3–39. [[CrossRef](#)]
14. Wang, J.; Zhou, S.; Zhang, Z.; Yurchenko, D. High-performance piezoelectric wind energy harvester with Y-shaped attachments. *Energy Convers. Manag.* **2019**, *181*, 645–652. [[CrossRef](#)]
15. Shah, M.M.; Mahmood, R.; Latif, U.; Uddin, E.; Munir, A.; Zhao, M.; Riaz, H.H. Experimental investigation of the wake of tandem cylinders using pivoted flapping mechanism for piezoelectric flag. *Ocean Eng.* **2024**, *310*, 118587. [[CrossRef](#)]
16. Abdelkefi, A. Aeroelastic energy harvesting: A review. *Int. J. Eng. Sci.* **2016**, *100*, 112–135. [[CrossRef](#)]

**Disclaimer/Publisher's Note:** The statements, opinions and data contained in all publications are solely those of the individual author(s) and contributor(s) and not of MDPI and/or the editor(s). MDPI and/or the editor(s) disclaim responsibility for any injury to people or property resulting from any ideas, methods, instructions or products referred to in the content.